Cloverite: Exploring the 30 Å Supercage for Advanced Materials Science Applications

R. L. Bedard,[‖] C. L. Bowes, N. Coombs,[⊥] A. J. Holmes,[‡] T. Jiang, S. J. Kirkby, P. M. Macdonald, A. M. Malek, G. A. Ozin,* S. Petrov,[†] N. Plavac, R. A. Ramik,[§] M. R. Steele, and D. Young

Contribution from the Advanced Zeolite Materials Science Group, Lash Miller Chemical Laboratories, University of Toronto, 80 Saint George Street, Toronto, Ontario, Canada M5S 1A1.
Received August 18, 1992

Abstract: The cubic network of 30 Å diameter supercages in the novel gallophosphate molecular sieve cloverite receives attention in this work because of its potential as a host in innovative host-guest nanochemistry aimed at advanced materials applications. A multiprong analytical approach (PXRD, TGA/DSC/TMA/MS, ^{1}H, ^{13}C, ^{31}P, ^{71}Ga, ^{129}Xe NMR, UV-Vis, FT-IR, Raman, physical adsorption) is employed to begin the exploration of the thermal and chemical properties of cloverite, as-synthesized with the quinuclidine template and following various post-synthesis treatments. The freezing out of guest motions (template/water) and/or a change in the space group of as-synthesized cloverite occurs around −57 °C. Removal of extraframework H_2O occurs in two barely resolved stages at 90 °C and 110 °C. At this stage the quinuclidine template exists predominantly in the protonated form. The dehydration event is reversible and has very little effect on the integrity of the cloverite framework. Acid-base titrations of dehydrated cloverite with anhydrous NH_3 and HCl at room temperature reveal the essentially neutral nature of both the P(OH) and Ga(OH) hydroxyl groups of the interrupted framework of cloverite. This is to be contrasted with defect hydroxides in cloverite which behave as Brønsted acid sites. However, all P(OH) and Ga(OH) groups can be selectively deuterated with D_2 at 240 °C and D_2O at room temperature, leaving the hydrogens on the quinuclidinium template effectively untouched. Xe gas can access the larger, but not the smaller, channel of cloverite, both as-synthesized and after dehydration at 150 °C. Three thermal events occur around 350 °C, 450 °C, and 550 °C in which the occluded template (25%, 70%, 100%) and framework hydroxyls (40%, 90%, 100%) are systematically depleted from cloverite, simultaneously with the evolution of quinuclidine cracking products, framework HF, and H_2O. At each of these stages, Xe gas can only gain access to the supercages, being excluded from the LTA/RPA channel system of cloverite. The proton on the quinuclidinium housed in the interrupted framework of cloverite appears to play a key role in the production of dehydroxylated-dehydrofluorinated and/or partially fragmented double four-rings, through the thermally induced loss of framework HF and H_2O over this temperature range. However, up until about 450–500 °C, the disruption of double four-rings appears to be localized and short-range in nature. It does not appear to significantly reduce the crystallinity of cloverite at the unit cell level or the framework microporosity of the material, the latter with respect to O_2 and *n*-hexane adsorption. This process continues up to 800 °C, with the unit cell maintained essentially intact, at which point one observes catastrophic breakdown of the cloverite structure. The collapsed material at this stage is X-ray amorphous, but around 850 °C it recrystallizes predominantly into the dense phase tridymite form of $GaPO_4$. Between 850 and 1050 °C the evolution of CO is observed, which is considered to arise from a carbothermal reduction of the gallophosphate by residual carbon. A transformation of $GaPO_4$-tridymite into predominantly $GaPO_4$-cristobalite occurs around 1000 °C. A sintering transition begins around 1090 °C. Clearly the unit cell of cloverite remains essentially intact up until around 800 °C, although some short range disorder is introduced into the system up to this stage, most likely originating from the random production of disrupted double four-rings.

Introduction

The recent report by Estermann et al.[1] detailing the structure of a synthetic gallophosphate molecular sieve, "cloverite", with a 20 T-atom clover-leaf shaped entrance window leading into a supercage having a body diagonal length of around 29–30 Å has created great excitement in the molecular sieve community. Not all of the euphoria centers upon the potential unique adsorption and catalytic properties of this very large pore material and the possibility of producing other large pore sieves from this synthesis system. The generous dimensions of the cloverite supercage clearly also make it a promising new host for the encapsulation of semiconductor nanoclusters of larger dimensions than those prepared utilizing the void spaces currently offered by known zeolite and zeotype molecular sieve hosts.[2]

Considerable effort has been expended within our laboratory to prepare a series of novel materials called endosemiconductors (semiconductor cluster arrays, expanded semiconductors), anticipated to have exciting, device-oriented, optical, and electronic properties.[3] Endosemiconductors are prepared by assembly of the atomic components of bulk semiconductors within crystalline porous hosts to yield periodic arrays of monodisperse clusters. The valued optical and electronic properties alluded to above strongly depend upon the degree of spatial, quantum, and dielectric confinement conferred upon the clusters by the host material.[4] To date the principal host employed has been zeolite Y, a material having a diamond-shaped network of 13 Å supercages. The extreme degree of spatial confinement imparted by this host has resulted in the formation of clusters whose dimensions usually fall below those which can be readily dealt with using the tenets of theoretical solid-state physics, size quantization, and the effective mass approximation.[5] As a result of this, most contemporary evaluations of the potential of zeolites as new materials in, for example, quantum electronics, nonlinear optics, and photonics, point to the small cavity size (in comparison to polymer, porous glass, micelle, Langmuir-Blodgett film and protein hosts, for instance[6]) as being the major limiting factor. Utilization of a

[†] Ontario Geological Survey, 77 Grenville St., Toronto, Ontario, M7A 1W4 Canada.
[‡] Current address: Shell Research Ltd., Thornton Research Centre, Chester, England, U.K.
[§] Royal Ontario Museum, 100 Queens Park, Toronto, Ontario, M5S 2C6 Canada.
[⊥] Imagetek, 87 Robert St., Toronto, Ontario, M5S 2K4 Canada.
[‖] UOP, Tarrytown Technical Centre, Old Saw Mill River Rd., Tarrytown, NY 10591.

(1) Estermann, M.; McCusker, L. B.; Baerlocher, C.; Merrouche, A.; Kessler, H. *Nature* **1991**, *352*, 320.
(2) Ozin, G. A.; Kuperman, A.; Stein, A. *Angew. Chem.* **1989**, *101*, 373. Stucky, G. D.; MacDougal, J. E. *Science* **1990**, *247*, 669.
(3) Ozin, G. A.; Kirkby, S.; Meszaros, M.; Özkar, S.; Stein, A.; Stucky, G. D. Materials for Non Linear Optics. In *ACS Symposium Series*; Marder, S. R., Sohn, J. E.; Stucky, G. D., Eds.; 1991; Vol. 455, p 554.
(4) Wang, Y. *Acc. Chem. Res.* **1991**, *24*, 133. Steigerwald, M. L.; Brus, L. E. *Acc. Chem. Res.* **1990**, *23*, 183.
(5) Jaros, M. *Physics and Applications of Semiconductor Microstructures*; Clarendon: Oxford, 1989.

0002-7863/93/1515-2300$04.00/0

molecular sieve such as cloverite as a 3-D host, with a cubic network of 29–30 Å supercages, completely changes this situation and could therefore be extremely beneficial to research efforts in this area. The main purpose of this paper is to assess the physicochemical properties of cloverite pertinent to its utilization for host–guest inclusion chemistry aimed at advanced materials science applications.

Experimental Section

Synthesis. The relative molar composition of the reaction mixture used for the preparation of cloverite was as follows:

$$Ga_2O_3:P_2O_5:6\ \text{quinuclidine}:0.75HF:70H_2O$$

A typical synthesis procedure is outlined below. The reactor type used in our studies was a 16-mL capacity Teflon liner encapsulated in a stainless steel jacket (designed and constructed at the University of Toronto). $Ga_2(SO_4)_3{\cdot}8H_2O$ (2.37 g) [Strem] was weighed into the Teflon liner and dissolved with 2.40 g of deionized H_2O. H_3PO_4 (0.95 g) (85%) [Fisher] was then diluted with 0.95 g of deionized H_2O, added to the gallium sulfate solution and stirred well. No gel formed at this point. HF (0.13 g) (48%) [Caledon] was incorporated into the $GaPO_4$ reaction mixture and stirred for 1 h. Quinuclidine (2.76 g) [Fluka] was then added and a gel formed immediately. After rinsing down the liner walls with 0.84 g of deionized water, the reaction mixture was stirred for a further 2 h to ensure homogeneity. The reactor was then assembled and heated at 150 °C for 21.5 h. The initial pH of the reaction mixture was recorded as 3.2; the final value was 2.7.

Characterization. Elemental Analysis. Fluoride ion was analyzed by steam treatment of the sample at 1000 °C, with added V_2O_5 catalyst, and the HF obtained in this way was collected in dilute base followed by a selective electrode titration with NIST standards. Gallium was determined in an EDTA titration, with the colorimetric endpoint given by xylenol orange. Phosphorus was analyzed by inductively coupled plasma emission spectroscopy and carbon, hydrogen, and nitrogen with a standard C, H, N analyzer.

Powder X-ray Diffraction. The PXRD patterns were obtained with Phillips APD 1820 and APD 1730 powder diffractometers using either Cu or Co Kα radiation. The samples were ground to a fine powder and then spread onto a sample holder for collection of PXRD data. Pressing and back-filling techniques were also employed. Powder pattern simulations were generated using the POWD 12 program. A high-resolution powder pattern was also obtained using a Nonius Guinier de Wolff focusing camera with Cu Kα radiation.

Thermal Analysis. TGA and DSC analyses were performed using Perkin-Elmer TGA7 and DSC7 instruments, respectively, under both nitrogen and air atmospheres, with heating rates from 1–20 °C/min. Thermogravimetric-coupled mass spectroscopy analysis (TG-MS) was carried out to 1100 °C with a Mettler TA1 thermoanalyzer coupled to an Inficon IQ200 quadrupole mass spectrometer at a heating rate of 10 °C/min under vacuum, following the procedures given by Wicks and Ramik.[7] Thermomechanical analysis was conducted on a Orton 1500 recording dilatometer.

Adsorption Measurements. Isotherms were obtained with a McBain-Bakr system on a cloverite sample activated under vacuum at 450 °C.

Analytical Electron Microscopy. Scanning electron microscopy with energy dispersive X-ray fluorescence analysis (SEM-EDX) was performed on a Hitachi S-570 SEM using accelerating voltages from 5–25 kV and a Link AN1000 EDX system, using internal standards for quantitative elemental analysis.

^1H, ^{13}C, ^{31}P, ^{71}Ga and ^{129}Xe NMR Spectroscopy.[18] MAS-NMR spectra of ^1H, ^{13}C, and ^{31}P nuclei in cloverite were recorded on a Chemagnetics CMX-300 instrument using spinning rates of 4–5.5 kHz. Chemical shifts were measured relative to $(CH_3)_4Si$ (^1H, ^{13}C) and 80% H_3PO_4 (^{31}P). A Varian XL-400 spectrometer, fitted with a variable temperature attachment, was utilized for ^{129}Xe measurements. In this case, the spectra were referenced by using dehydrated zeolite $Na_{56}Y$ (UOP, Tarrytown, NY, lot number 12074-33), equilibrated with 400 Torr Xe at room temperature, as an external standard. The singlet signal of this reference sample was calibrated to be at 79.9 ppm with respect to Xe gas at zero pressure. Samples were prepared for examination by heating under high vacuum and then equilibrating with xenon at 400 Torr for 30 min upon cooling to room temperature. In total, five sample pretreatments were employed prior to examination by ^{129}Xe NMR: heating under vacuum at 1 °C/min to (a) 50 °C (12 h at 50 °C), (b) 150 °C (60 min at 150 °C), (c) 200 °C (60 min at 200 °C), (d) heating under vacuum to 400 °C followed by 40 min at 400 °C in vacuum, 20 min in 700 Torr O_2, and 30 min evacuation at 400 °C, and (e) heating to 550 °C, 40 min at 550 °C, 20 min in 700 Torr O_2, and 30 min evacuation at 550 °C.

FT-Mid-IR Spectroscopy. Mid-IR spectroscopy was performed on a Nicolet 20 SXB FT instrument. Samples were lightly ground and pressed into self-supporting wafers at a pressure of 3000 psi. These disks were sealed in a vacuum cell which permitted in situ heat treatment and dehydration, gas adsorption, and IR spectroscopy. Deuterium and anhydrous HCl were used as supplied by Matheson and Canadian Liquid Air. Ammonia from Matheson was dried over sodium metal before use. Deuterated water was 99.8 atom % ^2H, supplied by Aldrich (Gold Label), and was handled under nitrogen.

Raman Spectroscopy. Laser Raman spectra were obtained under ambient conditions on a Ramanor U1000 spectrometer (Instruments S.A.), equipped with a double monochromator (Jobin-Yvon, f = 1.0 m). An Ar^+ ion laser (Coherent Innova 90, λ = 514.5 nm), capable of delivering up to 700 mW at the sample, was employed. The laser plasma lines were removed using a monochromator (Spex 1460, f = 0.14 m). The sample was loaded as a powder in a glass capillary tube and mounted on an xyz translation stage for examination. Data were collected, and the cloverite spectrum baseline was corrected using a proprietary software package (Instruments S.A., U505.85.910).

UV–Visible Reflectance Spectroscopy. Optical diffuse reflectance measurements were recorded using a Perkin-Elmer 330 spectrophotometer adapted with an integrating sphere and linked to a personal computer to digitize the spectra. Spectra were referenced with respect to $BaSO_4$. Absorption spectra were calculated using a Kubelka-Munk transformation of the reflectance data.

Molecular Graphics. The cloverite structure was modeled using CHEM-X software and produced and sold by Chemical Design Ltd., Oxford, England and implemented on a Vaxstation 3200 computer.

Results and Discussion

Chemical Composition and Morphology of Cloverite Crystals. The elemental analysis (wt%) of the as-synthesized cloverite produced the following composition:

Ga_2O_3	P_2O_5	F	C	N
39.90	30.70	1.64	7.15	0.99

This yields the stoichiometry $Ga_{774.1}P_{761.9}O_{2976}(QF)_{153.4}$, to be compared with the reported *Fm*3*c* ideal unit cell formula $Ga_{768}P_{768}O_{2976}(OH)_{192}(QF)_{192}$.[1] The SEM micrographs (Figure 1) show the presence of well formed cubic crystals of cloverite up to 15μ in size. The Ga:P ratio is found to be close to 1:1 by EDX analysis. Also, EDX showed no evidence for any residual sulfate impurity.

The Structure of Cloverite. An understanding of the detailed structure of the cloverite molecular sieve is required in order to fully appreciate the results of the diffraction, spectroscopy, thermal, and chemical studies reported in this paper. These studies are greatly aided by the single crystal X-ray structure refinement of cloverite reported by Estermann et al.[1]

The asymmetric unit of cloverite contains 31 unique atomic positions (excluding quinuclidine and protons). Eleven of these are special positions, giving occupancies of 0.5. The formula for the asymmetric unit is therefore:

$$Ga_4P_4O_{16.5}F$$

Allowing for one quinuclidine molecule per F^- ion, terminal O atoms present as –OH, and a multiplicity of 192, the unit cell is therefore:

$$Ga_{768}P_{768}O_{2976}(OH)_{192}(QF)_{192}$$

This gives eight tetrahedral atoms (T-atoms) per fluoride, i.e., one F^- for each double four-ring (D4R). There are two types of D4R present in the structure, one type is fully coordinated involving apex oxygen bridged TO_4 units, while the other has $TO_3(OH)$ units bearing two adjacent terminal –OH groups, namely P(OH) and Ga(OH). The number of –OH groups indicates one hydroxyl group per fluorine, therefore leading to the conclusion that half of the D4Rs are not fully connected, yielding what is referred to as an interrupted framework for cloverite.

(6) Ozin, G. A. Nanochemistry: Synthesis in Diminishing Dimensions. *Adv. Mater.* **1992**, *4*, 612.

(7) Wicks, F. J.; Ramik, R. A. Vacuum Thermogravimetric Analysis and Evolved Gas Analysis by Mass Spectrometry. In *CMS Workshop Lectures, Vol. 3, Thermal Analysis in Clay Science*; Stucki, J. W., Bish, D. L., Mumpton, F. A., Eds.; The Clay Mineral Society: Boulder, Colorado, 1990; pp 159–189.

Figure 1. SEM data for as-synthesized cubic cloverite.

Table I. Channel Dimensions in Cloverite

channel	atom1···atom2	free diameter (Å)
20 T-atom	O19···O19	6.14
	O18···O18	6.03
	H1···H1	5.28
	H2···H2	5.46
8 T-atom	O5···O5	3.82

There are five crystallographically distinct types of Ga and P atoms in the unit cell, distributed according to

$$P1:P2:P3:P4:P5 = 1:0.5:0.5:1:1$$

$$Ga1:Ga2:Ga3:Ga4:Ga5 = 1:1:1:0.5:0.5$$

P3 and Ga5 are bonded to terminal hydroxyl groups. The structure of cloverite can be built exclusively from layers of D4R units, and therefore each P and Ga is included in a D4R and in intimate contact with a fluoride ion. The D4R units are in fact distorted, producing effectively five-coordinate Ga with distorted GaO_4F trigonal-bipyramidal geometry and Ga–F distances ranging from 2.30 to 2.66 Å (leading to very large quadrupolar broadening in the solid-state gallium MAS-NMR spectrum of as-synthesized cloverite—see later[18]). The P atoms remain tetrahedral with P–F distances greater than 2.78 Å. There are two types of structural –OH groups, Ga5–O19–H1 and P3–O18–H2, present in a 1:1 ratio. These structural –OH groups are located in the 20 T-atom entrance windows leading to the supercage and effectively line the large channel system with an ordered array of surface hydroxyls.

Using CHEM-X, we estimated the free dimensions of the two major channel systems in cloverite. Figure 2 displays a CHEM-X representation of the unit cell of cloverite. Estermann et al.[1] quote a value of 6.0 Å for the free diameter of the 20 T-atom ring, using $r(O) = 1.35$ Å, the commonly accepted value for the effective radius of the oxygen atom in silicates. Table I lists the dimensions for the twenty and eight T-atom ring systems, calculated from a CHEM-X model using $a = 51.712$ Å, and allowing for the presence of protons on the terminal O atoms (the T–O–H angle

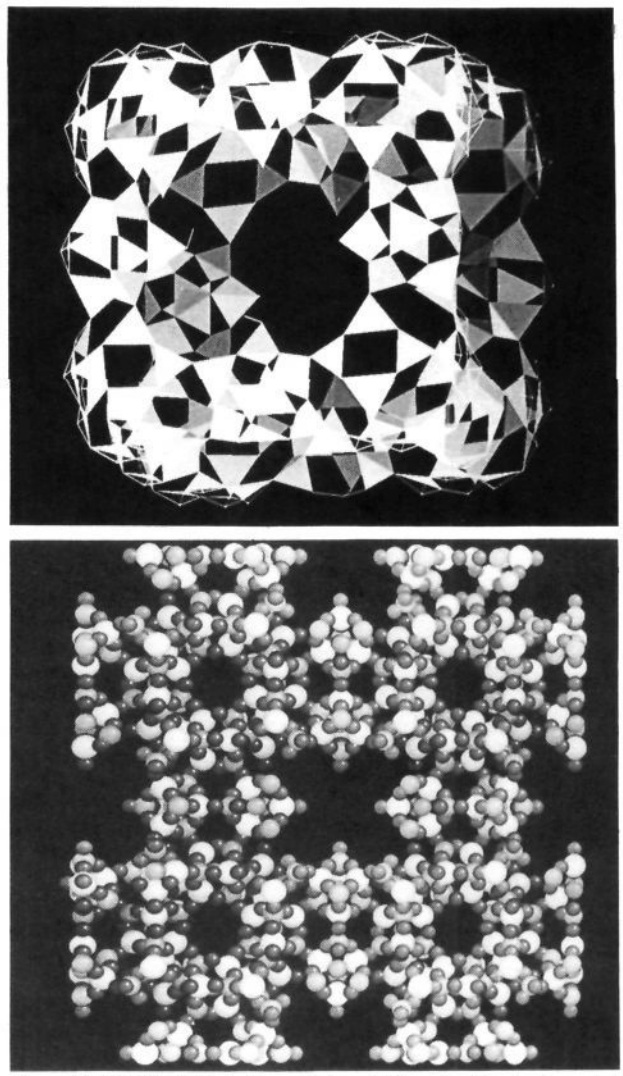

Figure 2. CHEM-X illustrations of cloverite based on the single-crystal atomic coordinates of framework Ga,P,O,F:[1] (A) (top) [100] projection of unit cell and (B) (bottom) the 29–30 Å supercavity.

was set to be the tetrahedral angle). Xe is expected to freely travel through the 20 T-atom ring system. However, in the case of the eight-ring, the free dimension is 3.82–3.89 Å suggesting that Xe with a kinetic diameter of 3.96 Å may not gain access at room temperature (see ^{129}Xe NMR later). It is worth noting that the only internal connection between the eight and 20 T-atom channel systems is via six T-atom rings!

Inspection of the cloverite structure shows that the crystallographically determined free dimension of the eight-ring window (ca. 3.9 Å) is somewhat smaller than that for zeolite 5A $Ca_4Na_4Si_{12}Al_{12}O_{24}$ (4.2 Å), which will sorb Xe. Breck quotes an "apparent" pore diamter, based on sorption data, of 4.2–4.4 Å.

Identification and Characterization of As-Synthesized Cloverite. The identity and purity of as-synthesized cloverite were established by PXRD. More than 355 reflections were observed in the diffraction pattern over the d-spacing range of 30–2.11 Å. Many of these are composed of overlapping peaks; however, 27 independent reflections from the first 40 were used for primary indexing and determination of the lattice symmetry, lattice type, and space group for cloverite. In what follows, we summarize our procedure, which leads us to believe that these peaks are consistent only with the F-type cubic supercell with a c-glide, but neither d- nor n-glides. The data provide support for the cell proposed by Estermann et al.,[1] which was found from a single crystal XRD study to be *Fm3c* (space group no. 226).

We followed the standard indexing procedure, which involves a step-by-step collection of all crystallographic information only

Table II. Relation between the Supercell (F) and Two Subcells (P and I) in Cloverite

		P cell, a = 25.8 Å		I cell, a = 36.5 Å		F cell, a = 51.6 Å	
no.	d, Å	N^a	hkl	N	hkl	N	hkl
1	25.78	1	100	2	110	4	200
2	18.28	2	110	4	200	8	220
3	14.93	3	111	6	211	12	222
4	12.94	4	200	8	220	16	400
5	11.58	5	210	10	310	20	420
6	10.55	6	211	12	222	24	422
7	9.149	8	220	16	400	32	440
8	8.615	9	300, 221	18	411, 330	36	600, 442
9	8.184	10	310	20	420	40	620
10	7.800	11	311	22	332	44	622

$^a N = h^2 + k^2 + l^2$.

from the available PXRD pattern. The first 40 reflections in the pattern, ranging from 30–3.60 Å, were carefully measured and corrected using Fluorphlogopite (NBS Reference Material no. 675) as an internal standard. These were then used in the following procedure.

Stage I consists of using the first 10 peaks for primary indexing, to determine the lattice symmetry of cloverite. By using **a** versus **d** graphical techniques, the lattice symmetry is found to be cubic. Stage II consists of distinguishing the three types of cubic unit cells (supercell F and subcells P and I) which are related to each other as shown in Table II. The I-subcell was rejected because of existing reflections with d = 6.920 Å (N = 28) and d = 4.719 Å (N = 60), which cannot be indexed at all. The P-subcell was rejected because the peak with d = 4.148 Å also gives a forbidden value of N = 39. The only cell which could index all 40 reflections is the F-supercell. After an additional check using a list of all possible reflections for the F-supercell, the remainder of the first 80 peaks were successfully indexed. The **a** value was then calculated by the Appleman and Evans/Benoit refinement routine. The corrected d-space values of five well-shaped symmetrical peaks in the range 25° < 2θ < 40° (Cu Kα) were used. The value of a = 51.7114(78) Å so obtained, is close to that reported by Estermann et al.[1] Note that their reported value of 52.712 Å is a typographical error for the acceptable value of 51.712 Å.[8]

Stage III involves the most difficult problem of determining the space group. Usually, it is not possible to establish the space group by PXRD data alone. Fortunately, in the case of cubic symmetry, some special circumstances allow the identification of the main diffraction symbols. From all 36 possible cubic space groups, 25 can be automatically eliminated. Following the nomenclature of Donnay and Harker, one has to choose between 11 F-space groups of five types as follows:

F..... 5

F4$_1$... 1

Fd..... 2

F.....c 2

Fd....c 1

The presence of certain translation elements of symmetry narrow down the choice. Thus, the lack of a 111 peak shows the presence of c- and d-glides. The presence of the 200 and 420 peaks eliminates the possibility of d-glides. The choice is then between *F*43*c* (no. 219) and *Fm*3*c* (no. 226). These two space groups have equivalent diffraction diagnostics but can be distinguished by reference to the unusually low density of cloverite, which favors the less closely packed octahedral, centrosymmetric *Fm*3*c* arrangement over the more well packed tetrahedral, noncentrosymmetric *F*43*c* one.

A final check of the purity of the as-synthesized cloverite was undertaken by comparing the calculated and experimental PXRD patterns. The structural parameters of Estermann et al.[1] were used as input along with the partial (0.5) site occupancies of 5O, 2F, 2P, and 2Ga atoms. Two segments of the theoretical and

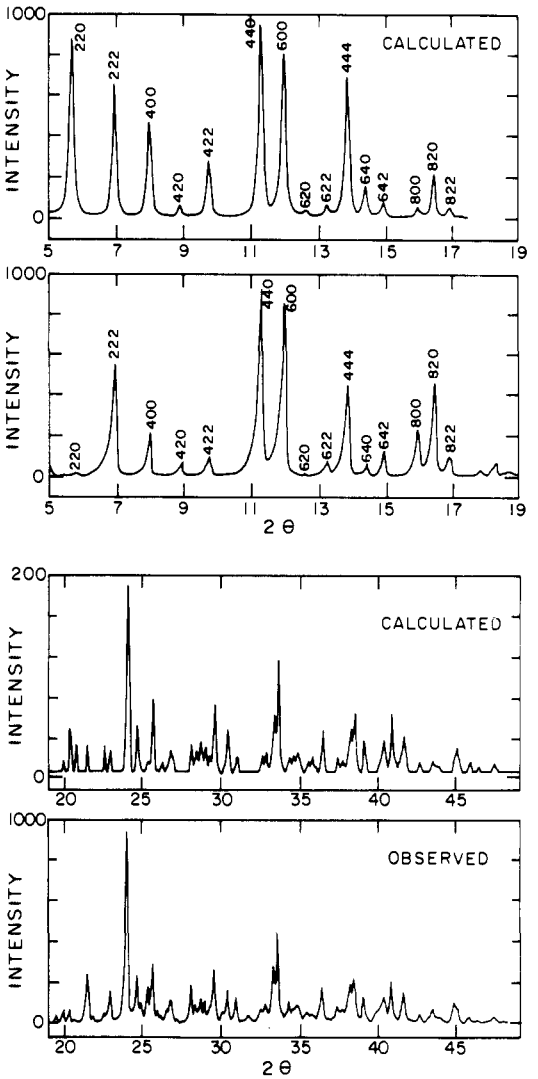

Figure 3. Observed and calculated Co Kα PXRD patterns for cloverite (5 < 2θ < 19 and 19 < 2θ < 49).

experimental cloverite PXRD patterns in different 2θ ranges are displayed in Figure 3. The close agreement serves to confirm the identity of the as-synthesized material as cloverite. The similarity of the PXRD to that more recently reported by Merrouche and co-workers[10] provides additional support for our proposals. The absence of extraneous peaks over the entire range of the PXRD pattern attests to the crystalline purity of the material. Note that the first peak (200, d = 25.8 Å) is missing in these figures because of the inability of the graphic output of POWD 12 to present data below 5° 2θ. A listing of the numerical output of the data for cloverite is presented in Table III.

Some significant discrepancies between the intensities and shapes of the first few peaks are found on examining closely the experimental and calculated PXRD patterns. The asymmetry

(8) Kessler, H., private communication.

Table III. XRD Powder Pattern of Cloverite (Low 2θ Range)

	experimental		calculated		
no.	d-space (Å)	intensity[a]	d-space (Å)	intensity[a]	*hkl*
1	25.78	18	25.86	>1000	200
2	18.28	2	18.28	86	220
3	14.93	50	14.93	63	222
4	12.94	18	12.92	47	400
5	11.58	6	11.56	6	420
6	10.55	9	10.56	27	422
7	9.149	100	9.141	100	440
8	8.615	90	8.618	82	600, 442
9	8.184	1	8.176	2	620
10	7.800	11	7.796	6	622
11	7.468	51	7.464	72	444
12	7.170	8	7.171	15	640
13	6.920	15	6.910	7	642
14	6.460	24	6.464	5	800
15	6.270	55	6.271	20	820, 644
16	6.096	10	6.094	5	822, 660
17	5.925	<1	5.932	<1	662
18	5.777	3	5.782	<1	840
19	5.639	8	5.642	<1	842
20	5.510	3	5.512	<1	664
21	5.278	3	5.278	1	844
22	5.172	5	5.171	2	1000, 860
23	5.070	5	5.070	4	1020, 862

[a] All calculated peak intensities are normalized with respect to the 440 peak to ease comparison with those from experimental data.

that occurs on all of the low θ peaks might be related to some lattice distortions and/or structural imperfections in cloverite, which is not unexpected for a material with such a huge unit cell and containing an interrupted framework (presence of terminal hydroxyl groups P(OH)OGa(OH) as an intimate part of the structure, rather than a framework consisting exclusively of four-connected tetrahedra).

The surprisingly low intensity of the first two experimental peaks (200 and 220) cannot simply be explained just in terms of preferred orientation effects, as a Guinier powder pattern (transmission diffraction) also shows their low relative intensities. The dramatic change of the $|F_{hkl}|$ values is in this instance possibly due to the presence of quinuclidinium template (NMR, IR, and Raman data for as-synthesized cloverite will be shown to favor dominance of the protonated over the neutral form of quinuclidine, see later) and/or extraframework water molecules located within the unit cell of the as-synthesized cloverite. These were not accounted for in either the single crystal structure determination or the powder pattern simulation. One probable scenario is that some of the protonated quinuclidinium and/or water molecules are located in the RPA cages, pockets in the 20-rings and pockets in the supercages (see later). This will cause the appearance of additional interplanes between (200) and (220) planes and could significantly decrease the intensity of both peaks. The higher order peaks, corresponding to the smaller interplanar d-spacings in the structure, would not be much influenced by this effect. This can explain the similarity between the calculated and observed PXRD patterns in the high 2θ range.

Thermal Analysis of Cloverite. Upon confirmation of the synthesis of cloverite as described above, several thermal analysis techniques (TGA/DTG/DSC/TMA/MS) were applied to study the effect of temperature, heating rate, vacuum, and different atmospheres on cloverite. A TGA/DTA study of as-synthesized cloverite has recently been published by Merrouche and co-workers.[10] Figure 4 displays the TGA/DTG trace for as-synthesized cloverite under N_2 with a heating rate of 1 °C/min. Four major weight losses are observed from room temperature to 900 °C. The first event, from room temperature to 200 °C, actually consists of two just resolvable stages, as observed in the DSC trace (Figure 5) and coupled TGA-MS (Figure 6). These are attributed

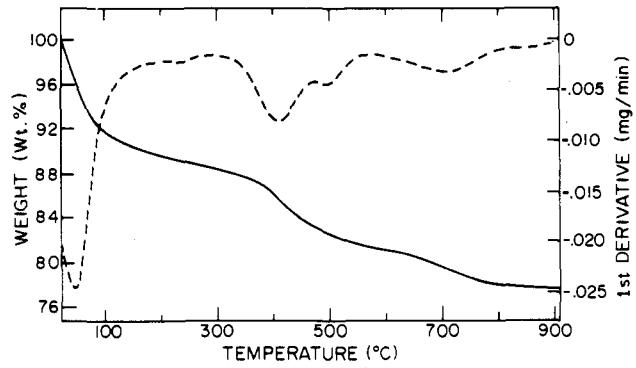

Figure 4. TGA/DTG trace of cloverite, run at 1 °C/min, under N_2.

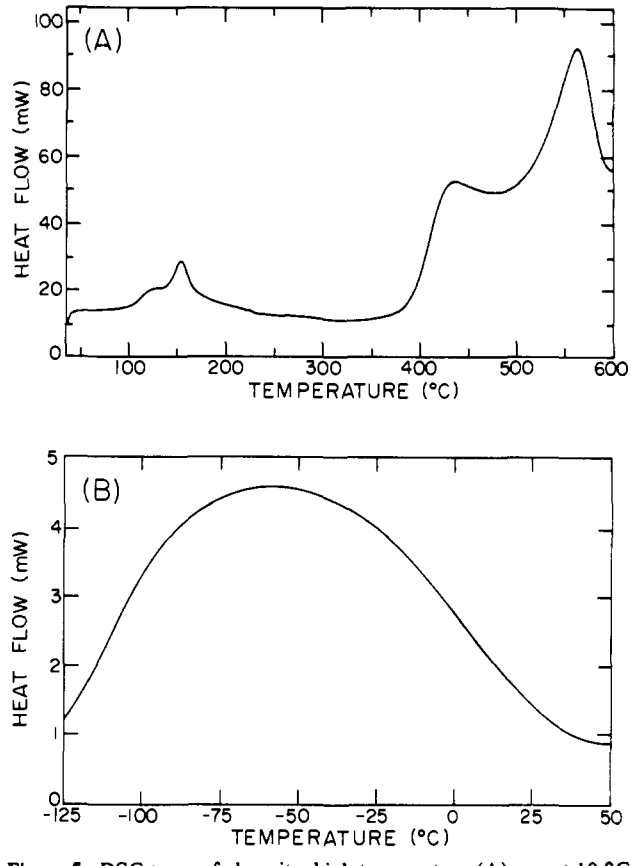

Figure 5. DSC trace of cloverite, high temperature (A) run at 10 °C/min, under N_2, and low temperature (B) heated at 20 °C/min under He.

to the loss of extraframework water from different sites in the cloverite lattice, from possibly physisorbed and chemisorbed states and/or supercage and LTA/RPA cage locations. Prolonged exposure to vacuum greatly reduces the first peak but leaves the second peak largely unaffected. No reduction in the structural integrity of the unit cell of cloverite was observed by PXRD upon dehydration. This is followed by the decomposition of quinuclidinium at higher temperatures accompanied by the evolution of H_2, small hydrocarbon pyrolysis products, HF and framework H_2O, as shown by coupled mass spectrometry. Maxima for these events occur at 410, 500, and 710 °C in N_2 (Figure 4) and at 315 and 460 °C in vacuum (Figure 6). The 410 °C event involves the loss of about one-half of the quinuclidinium, with simultaneous evolution of H_2O/HF. The latter are believed to originate from the cubic octomers that are part of the interrupted cloverite framework. PXRD shows the appearance of some short-range disorder (broadening and loss of intensity of higher angle diffraction peaks) but only a very slight loss of crystallinity at the unit cell level (low angle diffraction peaks). The next event at 500 °C is similar to the previous one. We postulate that at this elevated temperature, quinuclidinium is being pyrolyzed from the LTA/RPA secondary channel system of cloverite. This is evi-

(9) Turner, G. L.; Smith, K. A.; Kirkpatrick, R. J.; Oldfield, E. *J. Magn. Reson.* **1986**, *70*, 408.

(10) Merrouche, A.; Patarin, J.; Kessler, H.; Soulard, M.; Delmotte, L.; Guth, J. L.; Joly, J. F. *Zeolites* **1992**, *12*, 226.

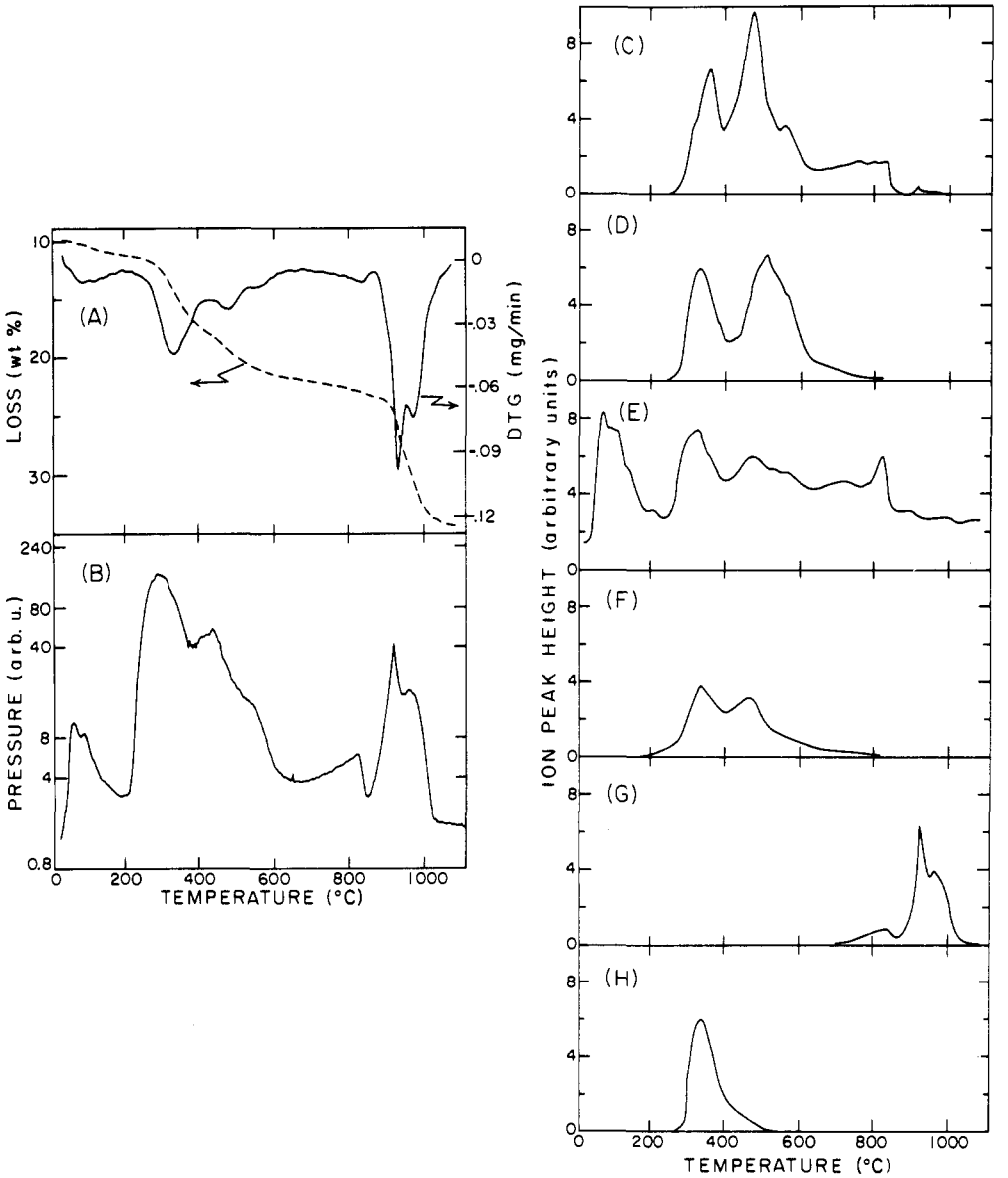

Figure 6. TGA-MS data for cloverite run at 10 °C/min under vacuum: (A) TGA/DTG (approximately 10% water loss due to sample evacuation was observed prior to run); (R) total ion mass spectrometry curve; selected ion mass spectrometry curves (C) m/e = 2, H_2^+, ×2; (D) m/e = 15, CH_3^+, ×20; (E) m/e = 18, H_2O^+, ∧20; (F) m/e = 20, HF^+, ×20; (G) m/e = 28, CO^+, ×1; and (H) m/e = 111, quinuclidine$^+$, ×100.

denced by the cessation of quinuclidine evolution and the renewed evolution of H_2 and smaller organic fragments (the latter exemplified by m/e 15 in Figure 6). The nature of the 710 °C event (in N_2) is uncertain as it does not correlate closely with TG-MS events (in vacuo). The latter data show rises in H_2O and H_2 evolution, which peak at 830 °C then abruptly cease. This correlates with the phase transition of cloverite to predominantly $GaPO_4$-tridymite detected by PXRD near 850 °C. TG-MS data between 850–1050 °C record the loss of CO and high mass volatiles including m/e 124, 156 and 172 (with high concurrant O^+), which may be interpreted as GaF_2O^+, Ga_2O^+, and $Ga_2O_2^+$ moieties, respectively. The CO loss likely arises from the oxidation of residual carbon, that is a carbothermal reduction of the $GaPO_4$-tridymite. If the 124 mass is indeed GaF_2O^+, it indicates that some fluorine is retained at high temperatures, even above the 850 °C transition. Interestingly, $GaPO_4$-tridymite converts to predominantly $GaPO_4$-cristobalite around 1000 °C (PXRD, see later).

These processes were also studied by TMA (thermomechanical analysis, specifically dilatometry). Dilatometry is a useful technique for studying the thermal behavior of microporous frameworks. A dilatometric experiment is carried out by heating a pressed pellet of a microporous powder in a furnace while the linear shrinkage of the pellet is monitored by a spring loaded piston coupled to a linear differential voltage transformer. Dilatometric data complement other thermal analyses such as TGA and DTA, giving valuable information on structure collapse of microporous frameworks. The thermal events observed in a DTA spectrum can often be completely assigned to specific processes by combining the dilatometric results with the TGA results.

Caution should be exercised during interpretation of dilatometric data and subsequent comparison with TGA and DTA data. The temperature scan rates of the different techniques should be the same. In addition, the pressed pellet form of the dilatometric sample is different from the sample form (loose powder) in the other thermal techniques. The sample form should always be kept in mind when interpreting thermal events, particularly when escaping gases can facilitate certain structural transformations (i.e., steaming effects or hydrothermal degradation).

A pellet of as-synthesized cloverite was prepared by loading approximately 0.5 g into a rectangular steel die and consolidating at 5000 psi. The pellet was loaded into a modified Orton dilatometer, and the temperature was ramped to 1200 °C at 6 °C/min in air.

There are six discernable slope changes in the shrinkage curve of cloverite, with inflection points at approximately 100, 150, 450, 770, 910, and 1090 °C (Figure 7). There is also a hint of a slope change at 300 °C that may have some significance in light of the

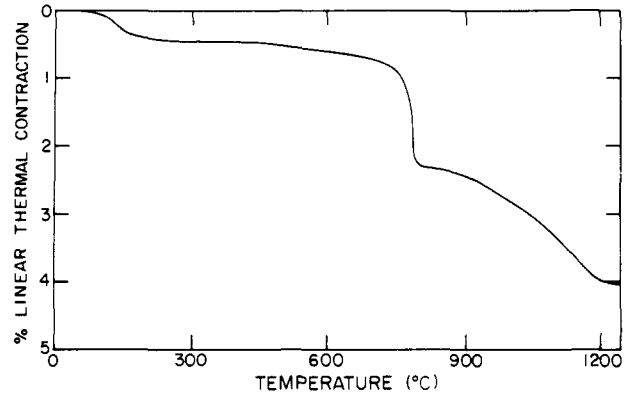

Figure 7. Dilatometry trace of cloverite, run at 6 °C/min in air.

other thermal analysis data. The small first shrinkage event (100–150 °C) is caused by the loss of water from accessible intracrystalline channels. The small second shrinkage process near 300 °C likely involves the loss of some of the quinuclidinium template and framework H_2O/HF. The slightly greater slope of the shrinkage that begins around 450 °C coincides with a slow degradation of the framework microporosity (see adsorption section), probably concomitant with loss of most of the remaining template. The large steep shrinkage event that follows around 770 °C corresponds to a rapid collapse of the remaining porosity in the individual powder grains and recrystallization to $GaPO_4$-tridymite. Carbothermal reduction and partial sintering of the powder begins around 910 and 1090 °C, respectively.

The total weight loss measured under N_2 at 900 °C is found to be 22.3 wt % and under air at 1000 °C it is 24.1 wt %. The weight loss at 200 °C under N_2, corresponding to the removal of extraframework water, is determined to be 10.26 wt %. This translates into roughly 973 H_2O per unit cell. This figure is believed to be somewhat in excess of the expected amount due to mainly extraframework water, owing to some contribution from framework dehydroxylation–dehydrofluorination. The weight loss from 200–900 °C found under N_2 is 12.04 wt % and from 200–1000 °C under air is 13.84 wt %. These are both less than the 17.53 wt % value expected for the removal of the 192 crystallographic unit cell equivalents of occluded quinuclidinium, framework HF, and H_2O. This 3.69–5.49 wt % discrepancy could originate from a number of different contributions including the deposition of carbon in the cloverite lattice from incomplete pyrolysis of the quinuclidinium template (see UV–vis, MS), there being less than the full 192 equiv of template, framework HF, and H_2O in the cloverite unit cell (see elemental analysis), and the incomplete removal of fluoride at high temperatures (see MS).

The interrupted framework, taken together with the proton on the void filling quinuclidine template, can be considered to play a key role in the creation of dehydroxylated–dehydrofluorinated and/or partially fragmented double four-rings, which initiates and eventually leads to the catastrophic breakdown of the cloverite lattice (see later).

In low-temperature DSC a broad endotherm was observed at ca. −57 °C, Figure 5. This most likely represents the freezing out of template/water guest motions and/or a change in the space group of cloverite.

Consolidation of the above data allows one to deduce that eight major thermal events exist during the heating of cloverite over the extended temperature range −150 °C to 1200 °C. The low-temperature one (−57 °C) involves occluded guest and/or lattice dynamical processes. Two intermediate events (90 and 110 °C) are most likely associated with loss of physisorbed and chemisorbed and/or supercage and LTA/RPA cage extraframework H_2O. The high-temperature ones (350, 450, 550 °C) encompass the loss of uncracked quinuclidine as well as the pyrolysis of quinuclidinium which is accompanied by the evolution of H_2, small organic fragments, HF, and structural H_2O. These latter events were accompanied by only a minor perturbation of structural integrity, until the cloverite underwent framework collapse starting around 770 °C, with more rapid structural breakdown starting around 800 °C, then recrystallized predominantly to $GaPO_4$-tridymite near 850 °C, experienced carbothermal reduction with residual carbon from about 910 °C, transformed to predominantly $GaPO_4$-cristobalite near 1000 °C, and then finally sintered from ca. 1090 °C.

Variable Temperature in Situ Powder XRD. The question of the extent to which framework integrity is maintained at various stages in the thermal treatments of cloverite is central to its evaluation as a host material for various applications. In order to address this in more detail, an in situ PXRD study of the thermal treatment of cloverite was performed. The results of this study are summarized in Figure 8. Following heating in N_2 at 50 °C for 60 min, the PXRD pattern is essentially unchanged. Upon heating to 200 °C for 60 min, at which stage most of the extraframework H_2O should be removed, a slight loss of structure in the higher angle peaks is observed. The PXRD pattern remains basically the same upon heating the sample to 450 °C. From 200 to 450 °C the TG-MS shows that loss of quinuclidine, HF, and H_2O is occurring. This situation is maintained at 550 °C. Incredibly, on reaching 750 °C most of the low angle PXRD intensity still persists and some loss of resolution of the high angle peaks is noticed, Figure 9. This situation does not change much up to 800 °C. The material recrystallizes to, predominantly, the dense-phase tridymite form of $GaPO_4$ around 850 °C and then transforms to, predominantly, the cristobalite form of $GaPO_4$ near 1000 °C. Samples heated in the range 200–750 °C show essentially no change upon cooling to room temperature and exposing to air for 1 h. Allowing these samples to stand in air overnight always leads to total framework collapse.

The in situ temperature dependent PXRD investigation of cloverite allows one to draw the following conclusions. Removal of extraframework H_2O causes minimal structure degradation. The gradual removal of the quinuclidinium template, together with framework HF and H_2O, over the range 200–550 °C causes some loss of short-range order but with the unit cell essentially intact. This situation does not change appreciably up to around 750–800 °C. Catastrophic breakdown of the cloverite lattice ensues around 800 °C, followed by a recrystallization to largely $GaPO_4$-tridymite at 850 °C, followed by conversion to mainly $GaPO_4$-cristobalite close to 1000 °C.

McBain Adsorption Studies of Cloverite. For a cloverite sample activated under vacuum at 450 °C, the adsorption capacity for oxygen (kinetic diameter, 3.46 Å) (−183 °C) at $P/P_0 = 0.4$ was 27.5 wt % (24.1 cc/100 g) and for *n*-hexane (kinetic diameter, 4.30 Å) at $P/P_0 = 0.5$ was 14.7 wt % (22.3 cc/100 g). The *n*-hexane adsorption capacity previously reported by Merrouche et al.[10] at $P/P_0 = 0.5$ was 15.8 wt %, in reasonable agreement with this study. It should be noted that the Merrouche et al.[10] adsorption experiment was carried out in a flow system with a binary N_2–adsorbate mixture. The McBain data from this study are therefore not strictly comparable to the reported adsorption behavior.

Interestingly, these values have both increased compared to a cloverite sample activated at 375 °C, where under the same experimental conditions the values for oxygen and *n*-hexane were 21.4 wt % (18.8 cc/100 g) and 12.4 wt % (18.8 cc/100 g), respectively. Presumably the enhancement of adsorption capacity of cloverite between 375 and 450 °C is due to the loss of additional quinuclidinium template. Apparently the slight disruption of the framework of cloverite over this temperature range, which likely involves random dehydroxylation–dehydrofluorination and/or partial fragmentation of the double four-ring (D4R) building blocks, does not adversely affect the framework microporosity of the material to any serious degree. Therefore, the adsorption results seem to be in line with the conclusions drawn from in situ temperature dependent PXRD, that the thermal treatment of cloverite in this temperature range introduces some degree of short range disorder into the framework but with the integrity of the unit cell remaining largely intact.

The *n*-hexane adsorption data reported by Merrouche et al.[10] are interesting in light of our data. Their results (14.9 wt % after

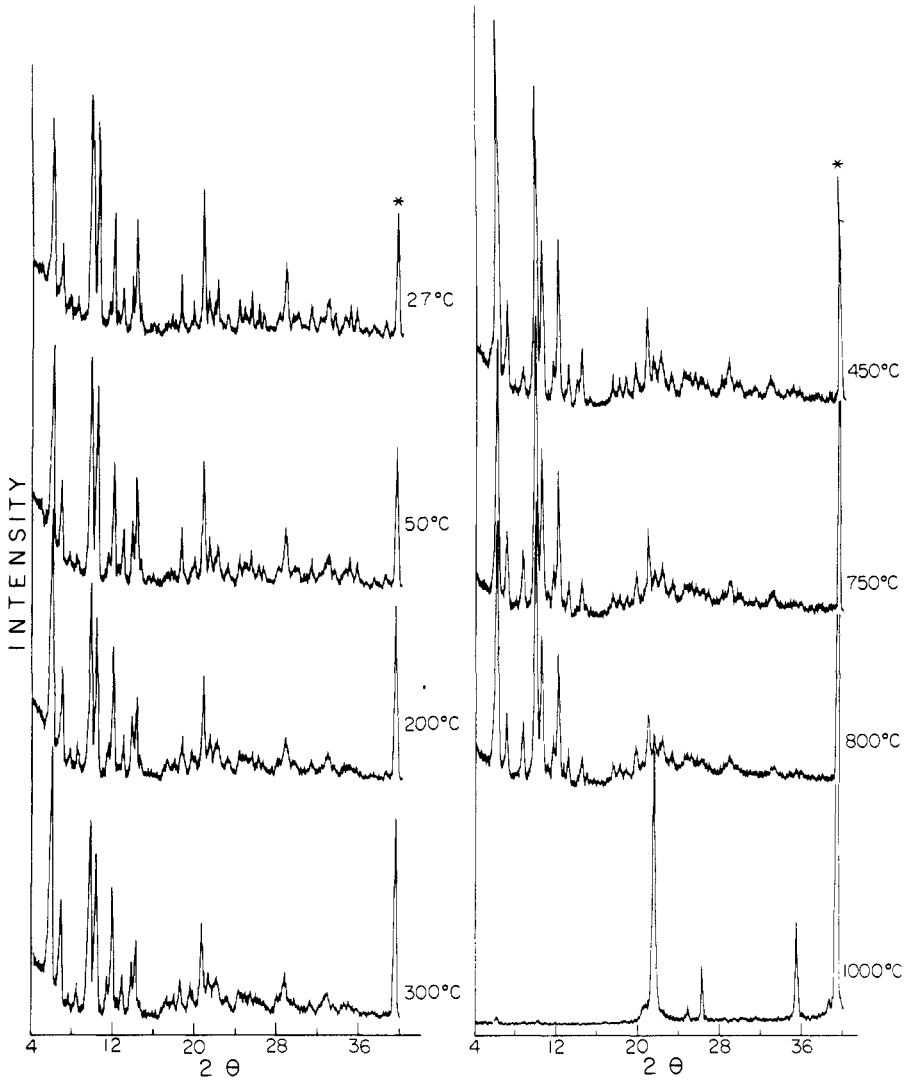

Figure 8. In situ temperature dependent PXRD study of cloverite (Pt strip heater, asterisk, N_2 atmosphere) run at 27, 50, 200, 300, 450, 750, 800, and 1000 °C.

380 °C activation, 15.8 wt % after 450 °C, 14.9 wt % after 500 °C, and 9.0 wt % after 600 °C activation) illustrate the process proposed here in which the removal of quinuclidinium, even with the introduction of short range disorder, improves the adsorption capacity of cloverite up until about 550 °C. Activation at higher temperatures appears to degrade the adsorption qualities of cloverite. This apparent degradation of microporosity up and above 600 °C could arise from a variety of causes, including pore blockage by extruded gallium oxo-species and/or increasing populations of disrupted double four-rings (see later).

NMR Studies of Cloverite. In this section, ^1H, ^{13}C, ^{31}P, ^{71}Ga and ^{129}Xe NMR spectroscopy is employed to study cloverite in the as-synthesized form as well as cloverite subjected to a range of thermal treatments.[18] Multinuclear site specific and environment-sensitive probes of this type provide valuable clues about the local structure and void spaces that exist in cloverite on removing extraframework H_2O, quinuclidinium template, and framework HF/H_2O from the crystal lattice. An NMR study of the as-synthesized cloverite has recently been reported by Merrouche and co-workers.[10]

^{31}P NMR Spectra of Cloverite. Hydrated Cloverite. The proton-decoupled ^{31}P MAS-NMR spectrum of as-synthesized cloverite is shown in Figure 9A. The peaks (ppm) observed are determined to be around

−2.6 ppm (a) −4.7 ppm (b) −9.9 ppm −11.4 ppm (c) −17 ppm

and are divided into three main groups (a, b, and c) for the purpose of the following discussion. To begin, the lowest field signals denoted (a) are closest to the chemical shift of an 85% solution of H_3PO_4 (0 ppm) and are best associated with the terminal hydroxyl group on P3. By comparison with the ^{31}P chemical shifts found for dense-phase isostructural metal phosphates, BPO_4 (−29.5 ppm), $AlPO_4$ (−24.5 ppm), and $GaPO_4$ (−9.8 ppm),[9] the most intense spectral feature (b) is assigned to the T-atoms P1, P2, P4, and P5. A third spectral feature (c), at higher field and of quite low intensity in hydrated cloverite, most likely originates from trace amounts of P=O groups.

The ratio of the integrated areas of the observed signals, a:b = 0.5:3.7, is very close to the crystallographic value of P3: (P1 + P2 + P4 + P5) = 0.5:3.5, and tends to confirm the above assignments.

The main spectral feature (b) always appears as a doublet and most probably consists of overlapping resonances from crystallographically-inequivalent phosphorus atoms.

Cloverite Dehydrated at 150 °C. The proton decoupled ^{31}P MAS-NMR spectrum of dehydrated cloverite, Figure 9C, shows a broadening of the spectral lines and a relative enhancement in spectral feature (c), assigned to P=O groups. Under cross-polarization, only signal (a) is enhanced (Figure 9B), confirming its assignment to the hydroxylated P3 site. Assuming that the relative increase in (c) results from dehydroxylation of framework P3(OH) groups even at 150 °C allows one to estimate from the ^{31}P MAS-NMR the endpoint, x, of this process using

$$a:(b + c) = (0.5-x):(3.5 + x)$$

This yields $x = 0.206$ implying that around 40% of the P3(OH)

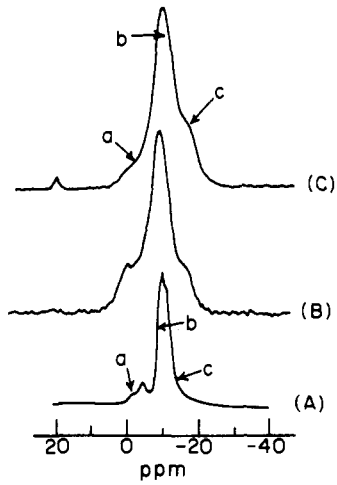

Figure 9. Solid-state ^{31}P NMR of cloverite: (A) as-synthesized MAS, (B) 150 °C, CP-MAS, CT = 0.25 ms, and (C) 150 °C, MAS proton decoupled. See text for discussion of signals denoted a, b, and c.

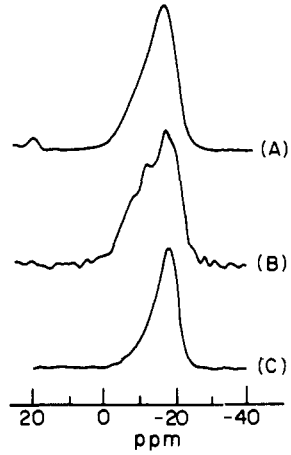

Figure 10. Solid-state ^{31}P NMR of cloverite: (A) 400 °C, MAS, (B) 400 °C, CP-MAS, CT = 0.1 ms, and (C) 450 °C MAS.

groups have been removed at 150 °C, forming P=O bonds (consistent with the mid-IR observations—see later). This should provide (a + c):b = 0.5:3.5, if the (c) signal is entirely P3=O groups produced from P3(OH). Assuming the same level of P=O impurities as in hydrated cloverite (0.081) leads to the ratio for the 150 °C dehydrated sample of (a + c):b = 0.5:3.42, thereby providing confirmation of the 150 °C partial dehydroxylation proposal. One can now appreciate the likely origin of the broader lines in the 150 °C dehydrated sample as arising from an inhomogeneous distribution of phosphorus T-atom microenvironments, due to the random placement of terminal P3=O/P3(OH) groups in the unit cell of cloverite.

Cloverite Vacuum Thermally Treated at 400 °C and 450 °C. Heating cloverite at 400 °C releases quinuclidine, small organics, and H_2 together with structural HF and H_2O (see TG-MS). The ^{31}P MAS-NMR spectrum of this sample shows an intense broad resonance around −16.9 ppm, a partially resolved, structured weak downfield shoulder extending from around −4 to −12 ppm and a very weak downfield impurity peak around 20 ppm, Figure 10A. CP-MAS conditions appear to enhance spectral features both on the downfield and upfield sides of the main resonance, Figure 10B. This could arise from magnetization transfer involving numerous kinds of P(OH) and Ga(OH) groups of partially fragmented D4Rs generated at 400 °C in the cloverite framework (see TG-MS, PXRD). The sample heated at 450 °C shows a similarly broad and structured ^{31}P MAS-NMR signal centered around −18.2 ppm, Figure 10C. The gradual shielding effect observed for the framework P atoms on heating from 150 °C to 400 °C to 450 °C could be the outcome of the gradual removal of H_2O and HF from the framework of cloverite.

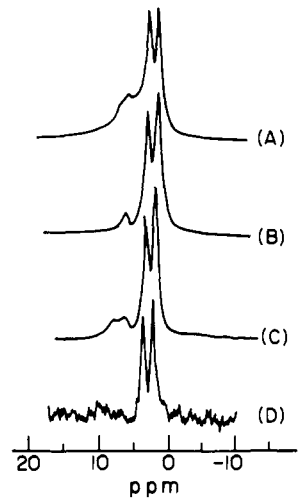

Figure 11. ^1H MAS-NMR of cloverite: (A) as-synthesized, (B) 150 °C dehydration, and (C) 400 °C (D) 450 °C.

^1H NMR Spectra of Cloverite. Hydrated Cloverite. The solid-state ^1H MAS-NMR spectrum of as-synthesized cloverite, Figure 11A, displays four signals around 7.6, 6.4, 3.4, and 2.0 ppm superimposed on a very broad background signal. After 150 °C dehydration, it is found that a room temperature rehydration process has essentially no effect on the ^1H MAS-NMR chemical shifts of cloverite. The solution-phase, high-resolution, ^1H NMR spectra of quinuclidine in D_2O (2.51, 1.52, 1.33 ppm) and quinuclidinium in D_2O/HF (2.67, 1.51, 1.30 ppm) are very similar and display only small solvent effects (this study). Therefore, the two upfield intense signals of cloverite around 3.4 and 2.0 ppm, with relative intensities of about 6:7, are best assigned to C-H protons of the template, where the signal at 2.0 ppm presumably results from an overlap of the two expected high field peaks (6:1) of quinuclidinium (see mid-IR, Raman). The remaining weaker signals observed at 7.6 and 6.4 ppm together with the broad background signal must be due to terminal P(OH) and Ga(OH) groups, with extraframework H_2O. Presumably the proton signal of the quinuclidinium is broadened to disappearance through quadrupolar interactions with the quaternary nitrogen and/or exchange effects involving hydroxyl/water moieties.

Cloverite Vacuum Thermally Dehydrated at 150 °C. Following the removal of extraframework H_2O from cloverite at 150 °C, one observes a ^1H MAS-NMR spectrum displaying three well resolved signals at 6.4, 3.4, and 1.9 ppm, with a weak shoulder around 7.6 ppm, Figure 11B. The intensity ratio of the hydroxyl to quinuclidinium C-H protons is 0.6:13.0. These results support the earlier proposal that at least 40% dehydroxylation of cloverite occurs after a 150 °C thermal treatment, as evidenced by ^{31}P NMR. The hydroxyl protons decrease by about 40% on deuteration of the sample using a single 150 °C dehydration-room temperature D_2O rehydration-150 °C dehydration procedure.

Cloverite Vacuum Thermally Treated at 400 °C and 450 °C. The ^1H MAS-NMR of cloverite subjected to heating at 400 °C (Figure 11C) still shows four resolvable peaks at 8.0, 6.4, 3.4, and 2.0 ppm with an intensity ratio 2.1:13.0 for the first two and the last two peaks summed together. Clearly the process of partially removing quinuclidinium template and framework HF/H_2O from cloverite (TGA-MS) at 400 °C enhances the ratio of terminal P(OH)/Ga(OH) groups to occluded quinuclidinium, consistent with the deductions from the corresponding ^{31}P CP-MAS-NMR study, Figure 10, and indicative of the production of partially fragmented D4Rs in the framework of cloverite, bearing additional terminal hydroxyl groups. Following the 450 °C thermal treatment, Figure 12D, only very weak quinuclidinium C-H proton signals are observed at 3.8 and 2.3 ppm, corresponding to remnants of the template, most likely housed in the LTA/RTA channel system of cloverite, in accordance with TGA-MS and mid-IR data.

^{13}C NMR of Cloverite. As-synthesized and thermally treated cloverite always display the same well resolved room temperature

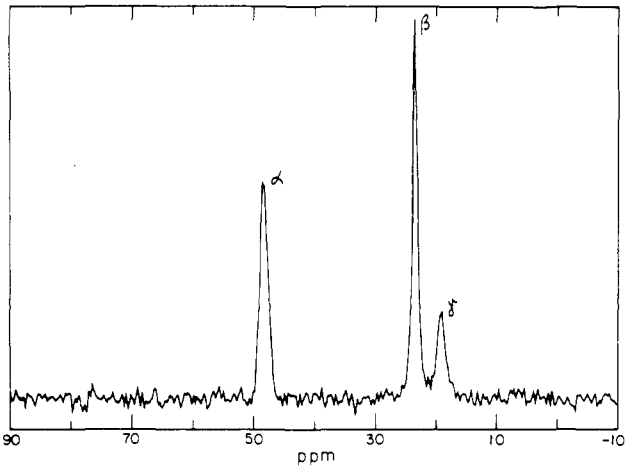

Figure 12. Proton decoupled ^{13}C MAS-NMR spectrum of as-synthesized cloverite. See text for discussion of signals labeled α, β, and γ.

^{13}C MAS-NMR spectra, Figure 12. The only effect is a monotonic decrease in the ^{13}C signal intensity of the α (48.5 ppm), β (23.4 ppm), and γ (19.1 ppm) carbons of the occluded template with increasing severity of the thermal treatment, paralleling the observations from mid-IR spectroscopy (see later). Essentially 90% of the intensity of the ^{13}C signal has disappeared in cloverite thermally treated at 450 °C. The solution-phase ^{13}C NMR spectrum of quinuclidinium in D_2O/HF shows peaks at α (47.3 ppm), β (22.8 ppm), and γ (19.2 ppm), whereas quinuclidine in D_2O shows them at α (47.0 ppm), β (26.0 ppm), and γ (20.7 ppm). In line with the conclusions drawn from mid-IR and Raman spectroscopy (see later), the template appears to exist predominantly in the protonated quinuclidinium form, thereby neutralizing the framework F^- housed in the double four-rings. Furthermore, on the time scale of the ^{13}C MAS-NMR experiment, motional dynamics of the template are likely responsible for the averaging of any site effects due to different locations of quinuclidinium in the unit cell of cloverite.

^{19}F NMR of Cloverite. The ^{19}F MAS-NMR spectrum reported by Kessler et al.[8] and Merrouche et al.[10] for as-synthesized cloverite shows a strong narrow line at −68.5 ppm (chemical shift reference, $CFCl_3$) which has been assigned to F^- anions located in the double four-rings (D4Rs) of the structure. With thermal treatment up to 450 °C, this ^{19}F signal (−71.5 ppm) shifts slightly upfield and simply decreases in intensity to about 15% of its initial value (consistent with the observed loss of ^{13}C MAS-NMR quinuclidinium intensity and mid-IR P(OH)/Ga(OH) ν(O–H) intensity), without the appearance of any other bands. This implies that the framework dehydroxylation–dehydrofluorination process, which causes slight loss of short-range order of cloverite at 450 °C (PXRD), involves the continuous loss of HF/H_2O (TGA-MS) from the double four-rings in unison with the loss of the quinuclidinium template.

^{71}Ga NMR of Cloverite. Static and MAS ^{71}Ga NMR spectra have been recorded on vacuum thermally treated cloverite at 150, 400, and 700 °C.[18] In brief, two very broad structured MAS-NMR resonances ($\Delta\nu_{1/2} \simeq$ 60–100 kHz) are observed for the 150 °C sample. These may correspond to gallium centers in the hydroxylated and nonhydroxylated double four-rings. The 400 °C sample shows a single, considerably narrowed resonance ($\Delta\nu_{1/2} \simeq$ 30 kHz) at an intermediate chemical shift value relative to the 150 °C sample. The static line width of the 400 °C sample is essentially the same as that under MAS conditions. This situation remains essentially unchanged for the 700 °C sample. These results are consistent with a distribution of gallium environments and/or a substantial quadrupole broadening in each sample which cannot be removed by MAS. ^{71}Ga DOR-NMR studies are underway in an attempt to improve the resolution of these samples.[18]

^{129}Xe NMR Spectra of Cloverite. All sample pretreatments yielded only one resonance in the ^{129}Xe spectra, Figure 13. The chemical shift for each sample (referenced against $Na_{56}Y$) is given in Table IV. Note that with pretreatment at successively higher

Table IV. Effect of Thermal Pretreatment on the Chemical Shift of Xenon Adsorbed in Cloverite at 400 Torr

pretreatment (°C)	chemical shift (ppm)	pretreatment (°C)	chemical shift (ppm)
50	74.4	400	24.6
150	59.1	550	20.3
200	53.6		

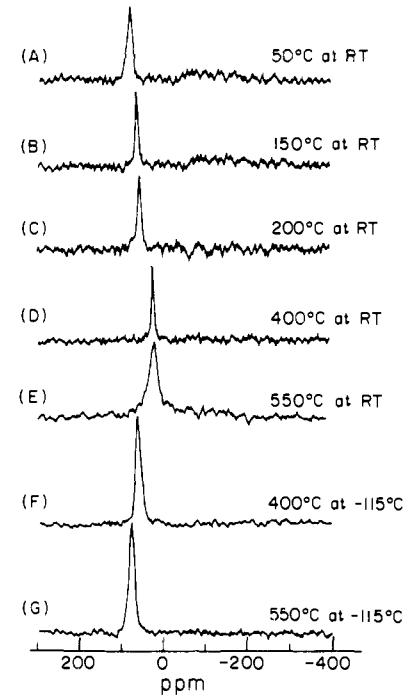

Figure 13. ^{129}Xe NMR of cloverite equilibrated with 400 Torr xenon and pretreated at (A) 50 °C, (B) 150 °C, (C) 200 °C, (D) 400 °C, and (E) 550 °C. Spectra recorded at room temperature and after cooling to −115 °C for samples pretreated at (F) 400 °C and (G) 550 °C.

temperatures, the signal monotonically shifts upfield, indicating a gradual increase in the free volume available to Xe.[11] The presence of only one signal might be interpreted to mean that Xe (kinetic diameter, 3.96 Å) only gains access to one of the channel systems of cloverite, presumably through the 20 T-atom ring window into the 29–30 Å supercage. The 400 °C and 550 °C pretreated samples were also cooled to −115 °C, in order to investigate the possibility of Xe traveling between the eight T-atom and 20 T-atom channel systems (possibly by intercrystalline transport) and giving rise to dynamic averaging of the Xe environment. Again only one resonance was observed, with the signal shifted downfield with respect to the room temperature sample, which is consistent with the enhanced sorption of Xe at the lower temperature. The fact that Xe does not appear to gain access to the eight T-atom ring channel system may be explained by reference to the estimated dimensions of the cloverite eight T-atom ring, Table I, as well as the likely constriction of this LTA/RPA channel system by pristine quinuclidinium template in the as-synthesized material as well as by residual carbonaceous products from the decomposition of the quinuclidinium template in the post-thermal treatment samples (TGA, UV-vis).

An increase in spectral line width of the Xe resonance in the sample treated at 550 °C (Figure 13) is probably due to inhomogeneous broadening effects arising from the random nature of the dehydroxylation–dehydrofluorination process (spatial effect).

The room temperature T_1 measured by the inversion recovery method for cloverite treated at 400 °C is 2.5s, which is considerably longer than the value of 0.041s recorded for dehydrated $Na_{56}Y$ under the same conditions. This is consistent with the location of Xe in the 29–30 Å supercage of the former compared to the 13 Å supercage of the latter. The T_1 value measured at 158 K shortens rather than lengthens, implying that, at room

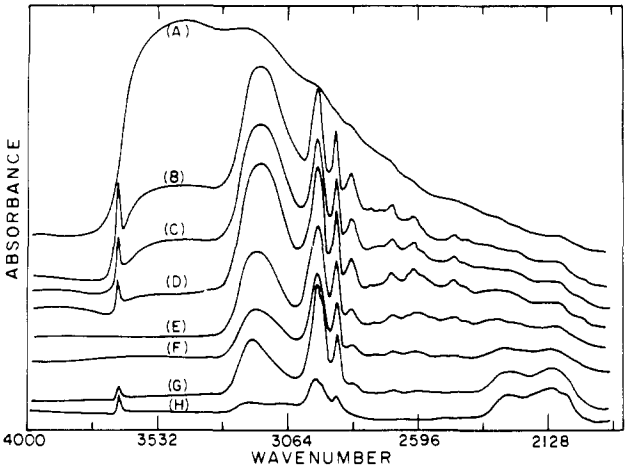

Figure 14. In situ mid-IR study of cloverite: (A) hydrated, (B) 60 °C, 2 h, (C) 100 °C, 2 h, (D) 170 °C, 2 h, (E) 300 °C, 3 h, (F) 375 °C, 3 h, (G) 415 °C, 2 h, (H) 450 °C, 2 h.

temperature, Xe is in the fast exchange mode. Much more work will be required to further quantify the ^{129}Xe NMR results.

In Situ Mid-IR Spectroscopy of Cloverite. The mid-IR spectra of cloverite, subjected to a range of thermal post-synthesis treatments, is extremely rich in detail concerning the dehydration of extraframework H_2O, the identity of the template (neutral or protonated form), the Brønsted acid–base behavior of the terminal hydroxyls P(OH)/Ga(OH), the template, and concomitant framework HF/H_2O removal process which leads ultimately to fragmentation of the D4Rs with collapse of the lattice structure of cloverite.

Dehydration of Cloverite. The outcome of a controlled in situ vacuum thermal dehydration of a cloverite self-supporting wafer over the temperature range room temperature to 170 °C can be appreciated from inspection of Figure 14. In essence, one can readily identify an intense, broad structureless band of extraframework H_2O centered around 3446 cm^{-1} which smoothly decays essentially to disappearance, leaving behind well resolved IR spectral features covering the range 3700–2000 cm^{-1}. By reference to the mid-IR spectra of quinuclidine and solid quinuclidinium chloride, Figure 15, one can readily identify a collection of bands in the range 3300–2000 cm^{-1} which appear to be diagnostic of the presence of quinuclidinium as the occluded template in cloverite. The Raman spectra support this proposal (see later). This leaves two bands centered around 3674 and 3163 cm^{-1} that are most likely associated with the OH stretching modes of terminal P(OH) and Ga(OH) hydroxyl groups. The former is weak and sharp and seems to fall in the region expected for "defect" hydroxyls (consider Si(OH), Al(OH), and P(OH) terminal groups and hydroxyl nests in all-silica, aluminosilicate, and aluminophosphate based zeolites and zeotype molecular sieves[12-14]), although one must wonder whether the interrupted framework of cloverite behaves as one "giant terminal hydroxyl defect" in this respect. The latter is strong, broad, and structured and falls in an IR region that could be attributed to the presence of the terminal P(OH)/Ga(OH) hydroxyl groups of the interrupted framework. About 50% of the intensity of the 3674-cm^{-1} defect feature is lost in the range 60–170 °C, whereas that at 3163 cm^{-1} remains little changed. The progression of mid-IR spectral changes over this temperature range can be seen by inspection of Figure 14. The major effect is the smooth decrease in the intensity ratio of the proposed P(OH)/Ga(OH) terminal hydroxyl band centered around 3163 cm^{-1} with respect to those assigned

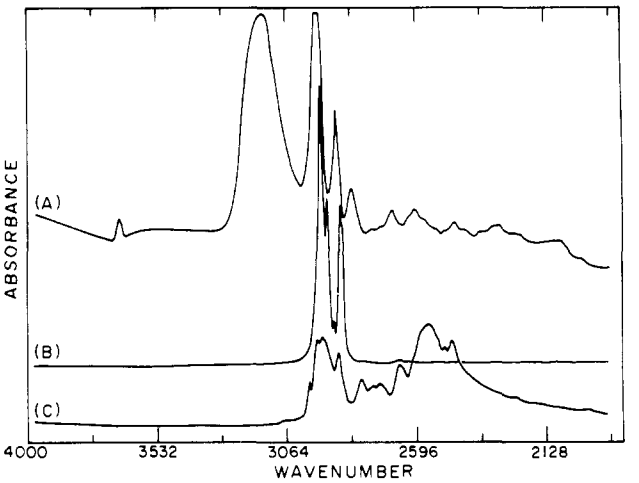

Figure 15. Mid-IR spectra of (A) 170 °C, 2 h dehydrated cloverite, (B) quinuclidine, and (C) solid quinuclidinium chloride.

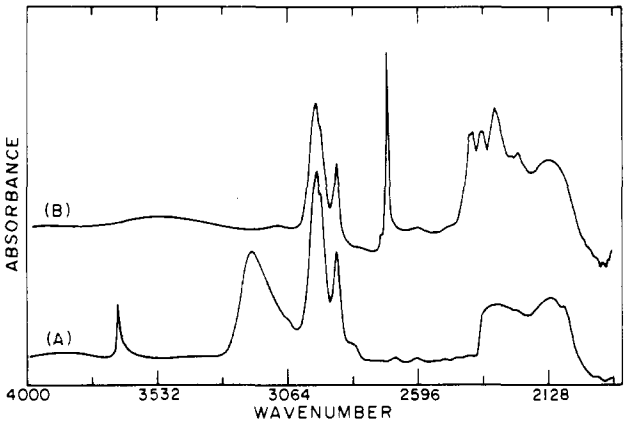

Figure 16. In situ mid-IR study of the deuteration of cloverite (A) dehydrated 2 h at 420 °C and (B) heated to 375 °C under 600 Torr D_2.

to the CH and NH fingerprint vibrations of the quinuclidinium template bands in the region 3000–2000 cm^{-1}, Figure 15. During this process the 3163-cm^{-1} band develops resolvable structure centered around 3117 and 3193 cm^{-1}. The weak defect hydroxyl band centered around 3674 cm^{-1} loses about another 50% of its intensity over this temperature range. One can estimate that approximately 30% of the terminal P(OH)/Ga(OH) hydroxyl intensity is lost by 170 °C, 70% by 375–415 °C, and more than 90% on reaching 450 °C, Figure 14. Under these same conditions, one can see that about 15%, 45%, and 80% of the quinuclidinium template has been removed from the unit cell of cloverite. These observations parallel those seen through the data of the corresponding TGA-MS and ^1H, ^{13}C, and ^{31}P NMR experiments. It would appear that the P(OH) and Ga(OH) interrupted framework functionalities both contribute to the broad structured mid-IR absorption centered around 3163 cm^{-1}. In order to confirm these proposals and at the same time gain some understanding of the Brønsted acid–base properties of this potentially "bifunctional" P(OH)OGa(OH) interrupted framework, titrations of these terminal hydroxyl groups with anhydrous D_2, NH_3, and HCl were attempted. The results of these investigations are summarized below.

Deuterium Exchange of Cloverite. The outcome of exposing various thermally treated samples of cloverite to 450 Torr of D_2 gas at temperatures in the range 170–420 °C has been probed by in situ mid-IR spectroscopy, Figure 16. Inspection of these data reveal that deuterium exchange is operative for both the defect and terminal hydroxyl bands at 3674 and 3163 cm^{-1} with observed $\sqrt{\mu OH/\mu OD}$ deuterium isotope shifts to 2709 and 2366 cm^{-1}, respectively. Throughout this OH/OD exchange process, the diagnostic CH and NH bands of the quinuclidinium template remain essentially unchanged. Interestingly, the broad structured

(11) Demarquay, J.; Fraissard, J. *Chem. Phys. Lett.* **1987**, *136*(3,4), 314. Barrie, P. J.; Klinowski, J. *Prog. NMR Spectrosc.* **1992**, *24*, 91.
(12) Ozin, G. A.; Ozkar, S.; McMurray, L. *J. Phys. Chem.* **1990**, *94*, 8297.
(13) Hunger, M.; Kaerger, J.; Pfeifer, H.; Caro, J.; Zidobrowius, B.; Bulow, M.; Mostowicz, R. *J. Chem. Soc., Faraday Trans. 1* **1987**, *83*, 3459.
(14) Barrer, R. M. *Hydrothermal Chemistry of Zeolites*; Academic Press: London, 1982; pp 261.

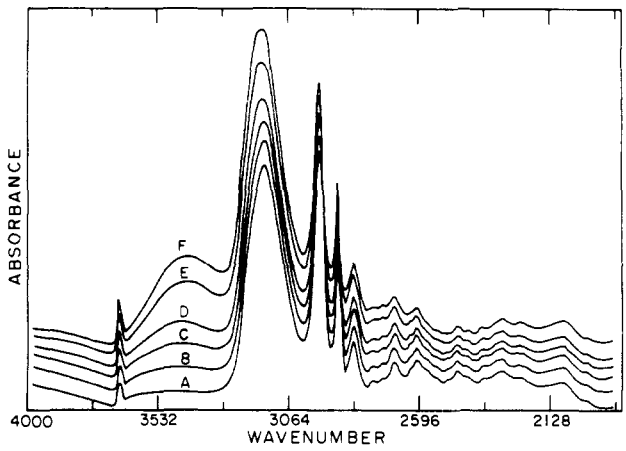

Figure 17. In situ mid-IR study of the room temperature titration of anhydrous HCl with 170 °C dehydrated cloverite (A) and (B–F) discrete additions of HCl.

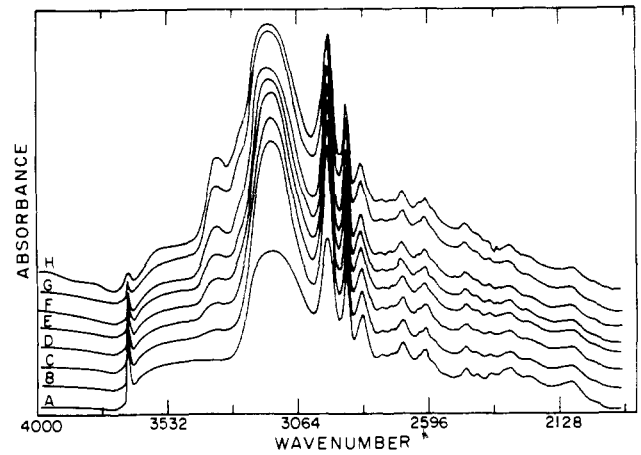

Figure 18. In situ mid-IR study of the room temperature titration of anhydrous NH_3 with 170 °C dehydrated cloverite (A) and (B–H) discrete additions of NH_3.

OH band around 3163 cm^{-1} shows resolved structure in its OD isotopically narrowed counterpart band around 2366 cm^{-1}, consistent with the idea that both terminal P(OH) and Ga(OH) ν(O–H) stretching modes (with superimposed vibrational site-splitting effects) are contained within this interesting mid-IR spectral feature. Similar mid-IR results are observed following a single 150 °C dehydration–room temperature D_2O rehydration–150 °C dehydration post-synthesis treatment, with the added effect that the broad featureless band of extraframework H_2O at 3163 cm^{-1} shifts to 2366 cm^{-1}, again revealing structure.

In Situ Mid-IR Study of the Room Temperature Titration of 170 °C Dehydrated Cloverite with Anhydrous HCl. The progression of such a titration is displayed in Figure 17. Surprisingly, rather than observing the consumption of a basic terminal hydroxyl group, one only observes the monotonic "growth" of the defect hydroxyl band around 3674 cm^{-1}, in unison with the growth and red shifting of a broad band around 3490 to 3450 cm^{-1}. All other bands remain essentially invariant throughout this titration. It therefore seems that the dominant effect of introducing anhydrous HCl into 170 °C dehydrated cloverite is for it to "seek-out" dehydroxylated framework functionalities according to the reaction

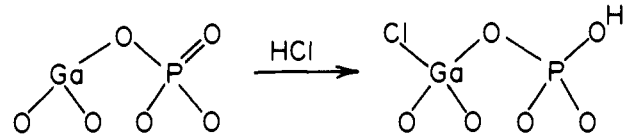

regenerating some terminal P(OH) groups and changing the three-coordinate gallium center to a four-coordinate one, Figure 21. Some hydrogen-bonding of HCl either to the P(OH) groups or to the oxygen part of the framework might be responsible for the band around 3450 cm^{-1}, by reference to work on proton loaded zeolite Y and $AlPO_4$-5.[12] It seems that at room temperature the Ga(OH) functionality is behaving as an essentially neutral hydroxyl group.

In Situ Mid-IR Study of the Room Temperature Titration of 170 °C Dehydrated Cloverite with Anhydrous NH_3. The progress of such a room temperature titration with incremental additions of NH_3 gas is documented in Figure 18. Here one can determine that the introduction of NH_3 depletes the defect hydroxyl OH band at 3674 cm^{-1}, concomitant with the growth of a broad band around 3360 cm^{-1}. All other spectral features remain basically invariant to the presence of NH_3. The best way to interpret these observations, with consistency maintained with all of the information presented in previous sections of this paper, is in terms of an acid–base reaction involving the defect hydroxyl with the

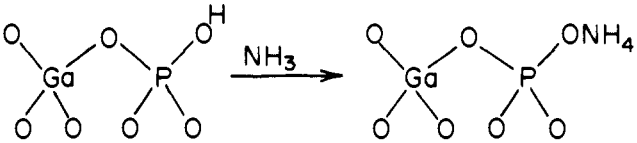

bands at 3674 and 3360 cm^{-1} ascribed to OH and NH stretching modes of the defect P(OH) and product NH_4^+ moieties, respectively.

Nature of the P(OH)/Ga(OH) Hydroxyl Groups of Cloverite. The results of the mid-IR study force one to conclude that at room temperature both P(OH) and Ga(OH) functionalities of the interrupted framework are behaving toward acids and bases like anhydrous HCl and NH_3 in an essentially neutral fashion. At first sight this may seem surprising but when one considers that these hydroxyls are part of the four-coordinate network of the cloverite oxide framework, then one can appreciate that the proton

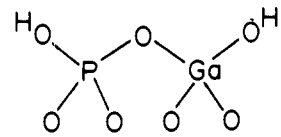

of the P(OH) group is not likely to be very acidic and that the hydroxide of the Ga(OH) group is unlikely to be very basic. Consider for comparison the very small value of the K_3 acidity constant of phosphoric acid. By contrast the defect P(OH) could be part of a hydroxide nest (Figure 18) and hence could display Brønsted acid properties as observed for cloverite. Additional studies will be required to explore the acid–base properties of cloverite at elevated temperatures.

Raman Study of Hydrated Cloverite. The Raman spectra of as-synthesized cloverite (A), quinuclidinium (B), and quinuclidine (C) are shown in Figure 19. These data indicate predominance of quinuclidinium over quinuclidine incorporated into the cloverite structure, as evidenced by the intermediate nature of the ν(C–H)/ν(N–H) stretching frequencies. This is further supported by the similarity of the ν_{sym}(C–N–C) modes between cloverite (618 cm^{-1}) and quinuclidinium (618 cm^{-1}) versus quinuclidine (605 cm^{-1}). It is interesting to note that the Raman intensities of the template modes overwhelm those of the gallophosphate framework modes, to the extent that one is hard pressed to unequivocally pin down many of the latter. One can identify unique cloverite framework modes at 194, 322, and 443 cm^{-1}. Consistent with this assignment of Ga–O–P framework modes in the gallophosphate cloverite is the fact that analogous Al–O–P modes in the aluminophosphate, VPI-5,[15] occur at higher frequency around 303, 375, and 488 cm^{-1}.

UV–Visible Reflectance Study of Cloverite. The optical properties of cloverite have been preliminarily assessed by studying the UV–visible reflectance spectrum of the material in the as-synthesized form and subjected to vacuum thermal dehydrations at 170, 350, and 400 °C and then calcined in oxygen at 400 °C. The hydrated and 170 °C dehydrated samples are essentially the same, showing what appears to be an oxygen to gallium/

(15) Holmes, A. J.; Young, D.; Kirkby, S. J.; Ozin, G. A. *J. Am. Chem. Soc.*, in press.

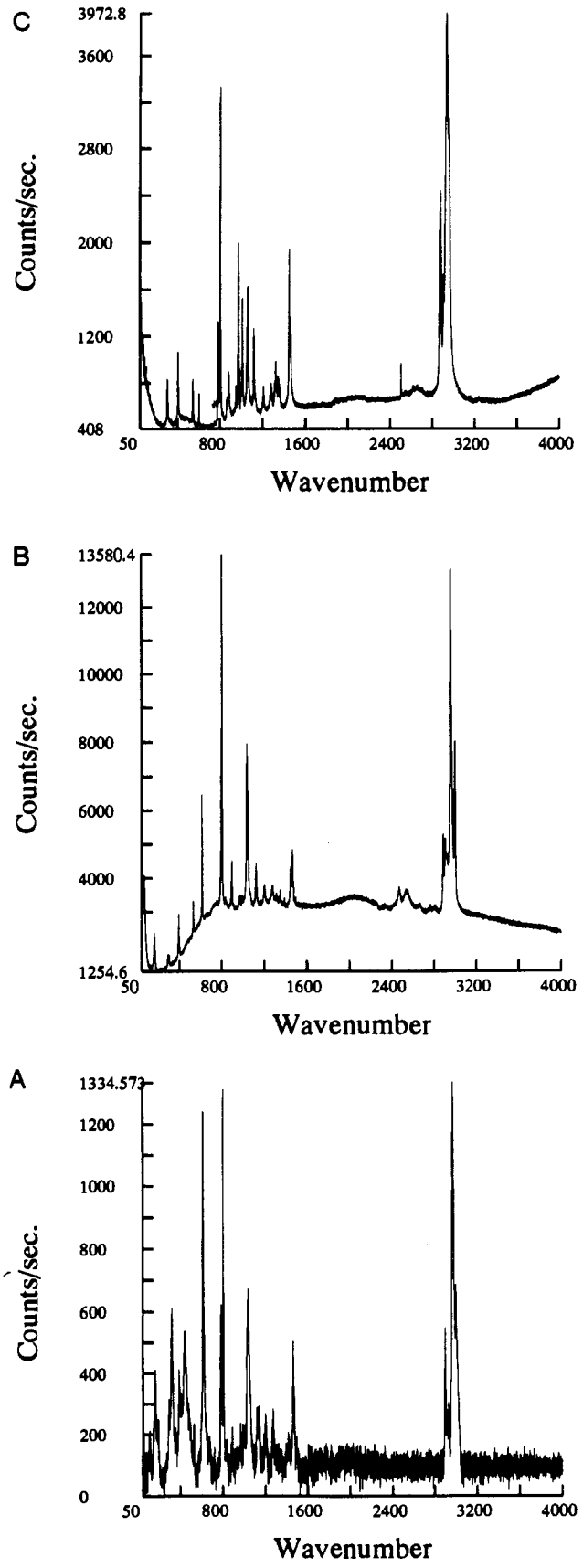

Figure 19. Raman spectrum of (A) as-synthesized cloverite, (B) solid quinuclidinium chloride, and (C) solid quinuclidine.

phosphorous ($O^{-II} \rightarrow Ga^{III}/P^{V}$) band-gap excitation centered around 250 nm, Figure 20. Surprisingly, at 350 °C an extraordinarily intense series of absorptions centered around 230, 275, and 340 nm emerge. These blue-shift to around 215, 250, and 315 nm on treatment of the sample at 400 °C. Calcination

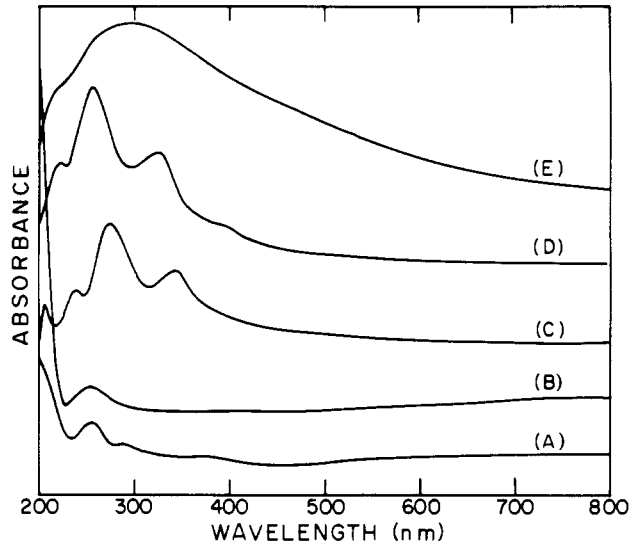

Figure 20. UV–visible spectra of cloverite samples thermally treated under different conditions (A) as-synthesized, (B) dehydrated at 170 °C, (C) 350 °C, (D) 400 °C, and (E) calcined at 400 °C.

of this sample at 400 °C transforms this intense spectrum into an equally intense one, centered around 300 nm, but with a width that encompasses most of the visible and UV range. Considerable work will be required to identify the species giving rise to these extraordinarily intense UV–visible excitations. One speculation is that they originate in π–π^* transitions of an occluded polycyclic aromatic,[16] resulting from the pyrolysis of the quinuclidinium template, perhaps even to buckminsterfullerene, C_{60}, as indicated by its UV spectrum (211, 256, and 328 nm in hexane[17]). ^{13}C NMR studies of this material as well as acid dissolution of the gallophosphate lattice and organic solvent extraction of the occluded carbon containing moiety are underway in our laboratory to explore this idea further.

Notes on the Formation of Cloverite and the Placement of 192 Quinuclidinium Cations in the Unit Cell. It is amusing to speculate on the mode of formation of such a high symmetry, exquisitely beautiful structure as cloverite. Inspection of the unit cell structure (Figure 2) shows that cloverite can be entirely constructed from layers of interlinked $Ga_4P_4O_{16.5}F$ cubic octomeric building blocks. One can imagine that the cloverite unit cell comes about from the self-assembly of 192$\{Ga_4P_4O_{12}(OH)_8F^- QH^+\}$ ion-pairs (where $QH^+ \equiv C_7H_{13}NH^+$, quinuclidinium cation) through a condensation–polymerization reaction of the fully hydroxylated cubane clusters, spatially directed by the QH^+ cation. Actually, the supercage of cloverite can be envisaged to arise from the creation of a massive, central, octahedral vacancy composed of seven of these cubane clusters (one cubane missing from the center of each of the six 20 T-atom windows, the remaining one gone from the center of the supercage). These "giant defects" can be considered to be responsible for the placement of 192 terminal Ga(OH)/P(OH) groups in the unit cell of cloverite. This creates two kinds of "proton pocket", a cubic-array of eight in each supercage and a square-array in each 20 T-atom ring window. In this way four distinct void spaces are created, and one can account for the location of 192 QH^+ cations in the fcc unit cell as follows:

$$8\ \mathrm{CLOV}(x8QH^+) = 64$$

$$8\ \mathrm{LTA}(x1QH^+) = 8$$

$$48\ \mathrm{RPA}(x\tfrac{1}{2}QH^+) = 24$$

$$24\ \text{20-RING}(x4QH^+) = 96$$

(16) Turro, N. J. *Modern Molecular Photochemistry*; Benjamin/Cummings Pub.: Menlo Park, CA, 1978.

(17) Aije, H.; Alvarez, M. M.; Anz, S. J.; Beck, R. D.; Diederich, F.; Fostiropoulos, K.; Huffman, D. R.; Krāschmer, W.; Rubin, Y.; Schriver, K. E.; Sensharma, K.; Whetten, R. L. *J. Phys. Chem.* **1990**, *94*, 8630.

(18) Jelinek, R.; Malek, A.; Ozin, G. A. (^{71}Ga solid-state NMR work in progress).

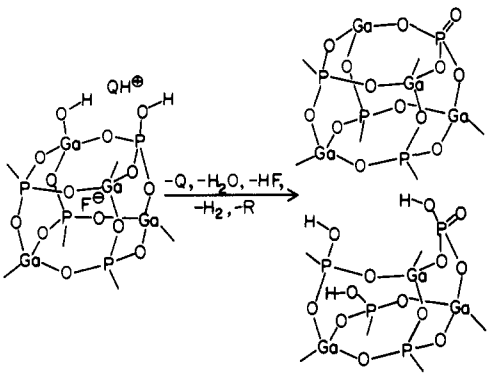

Figure 21. Double four-ring thermal chemistry of cloverite proposed to be responsible for the collapse of the interrupted framework: (top right) dehydroxylation–dehydrofluorination and (bottom right) partial fragmentation pathway.

This ideal model assumes that only one-half of the RPA cages are occupied by QH^+. If these QH^+ are unable to be removed in the pyrolysis or calcination procedures, then they could account for the observed QH^+ based carbonaceous residues in, and blockage of, the LTA/RPA eight T-atom ring channel system of cloverite. Recall that the elemental analysis of samples of as-synthesized cloverite indicate that less than the full, ideal crystallographic complement of QH^+ is actually present in the unit cell of hydrated cloverite.

Final Thoughts and Conclusions

The picture of the cloverite host and its solid-state chemistry that emerges from this study is quite detailed and rather encouraging at this stage, in terms of its potential for advanced materials chemistry and physics applications. Structurally, the system is best viewed as a 3-D cubic network of two distinct nonintersecting channel systems.[1] The smaller of these is accessed through eight T-atom rings and is lined with eight T-atom ring interconnected LTA and RPA cages. Entry to the larger occurs via 20 T-atom rings and is lined with interlinked cloverite supercages. The quinuclidine template exists in a predominantly protonated (IR, Raman) and dynamic (^{13}C NMR, DSC) form, within the cloverite lattice. Xe gas can access the larger but not the smaller channel system of as-synthesized cloverite at room temperature (^{129}Xe NMR).

Removal of H_2O occurs in two just distinguishable stages at 90 °C and 110 °C (TGA/DSC/MS) and is reversible, with little effect on the cloverite framework (in situ PXRD). This differential H_2O loss probably corresponds to different binding states and/or locations of extraframework H_2O in the cloverite and LTA/RPA channel systems, respectively. The supercage of cloverite under these conditions is lined with P(OH) and Ga(OH) terminal hydroxyl groups which appear to behave, at room temperature, as essentially neutral sites (in situ mid-IR probe of reactions with anhydrous NH_3 and HCl, respectively). These terminal hydroxyl groups and the defect hydroxyl groups can both be exchanged with D_2 gas at 240 °C and D_2O at room temperature. Xe gas is still only able to access the supercages of dehydrated cloverite at this temperature (^{129}Xe NMR).

The next thermal event occurs around 350 °C (TG-MS) and involves the loss of about one-half of the quinuclidinium, simultaneous with the evolution of some small organics, H_2 and HF/H_2O (mid-IR, NMR, TGA/DSC/MS). H_2 is likely produced by the pyrolysis of some of the quinuclidinium template. The HF/H_2O originates from those double four-rings that are part of the interrupted framework in the cloverite cage and is believed to form by the type of chemistry laid out in Figure 21. This event has very little effect on the crystallinity of cloverite at the unit cell level, but some short-range disorder is introduced due to the random production of dehydroxylated–dehydrofluorinated and/or partially fragmented double four-rings in the cloverite cage according to the idea illustrated in Figure 21 (in situ PXRD, NMR). Under such high-temperature conditions, one can envisage $Ga(OH)_3$ removal in an analogous fashion to that generally accepted for zeolite dealumination via steaming. Even at this stage, Xe gas can still only enter the supercages of cloverite (^{129}Xe NMR).

The next thermal event occurs around 450 °C (TG-MS) with a slight increase in framework microporosity (McBain) and involves the loss of more H_2, small organics, and HF/H_2O; this is most probably from the continuation of a process similar to the one that occurs at 350 °C. This step involves no further deterioration in crystallinity of the sample nor any further loss of short-range order (in situ PXRD). A less pronounced thermal event (vacuum TG-MS) occurs around 550 °C with the evolution of large amounts of H_2, most likely originating from pyrolysis of the remaining strongly bound quinuclidinium template probably residing and deposited in the LTA/RPA channel system. The lattice crystallinity remains essentially the same at this stage, although a slight deterioration in framework microporosity is observed (McBain).

One can appreciate from the above model how the interrupted framework, together with the protonated quinuclidine template, can be considered to be directly responsible for the creation of dehydroxylated–dehydrofluorinated and/or partially fragmented double four-rings, which leads eventually to catastrophic breakdown of the cloverite lattice around 770 °C with loss of additional H_2O (in situ PXRD, TGA/DSC/MS). At this stage, the collapsed material is amorphous but can be induced at 850 °C to recrystallize predominantly into the high-temperature tridymite phase of $GaPO_4$ (in situ PXRD). Between 850–1050 °C the evolution of CO and high mass volatiles, associated with species like Ga_2FO, Ga_2O, and Ga_2O_2 are observed. The CO loss is thought to arise from a carbothermal reduction of the gallophosphate support by residual carbon. $GaPO_4$-tridymite transforms to mainly $GaPO_4$-cristobalite close to 1000 °C (in situ PXRD). The material sinters around 1090 °C (Dilatometry). Clearly the unit cell of cloverite retains its integrity up until around 750–800 °C, although some short-range disorder is introduced into the system at this stage, owing to the random production of partially fragmented and/or dehydroxylated–dehydrofluorinated double four-rings. It is absolutely amazing how the unit cell of cloverite stands up, with the fluoride depleted from most of its double four-rings and the majority of the P(OH)OGa(OH) dehydroxylated to P(O)OGa groups. Experiments on cloverite are continuing, especially those aimed at further stabilization of the structure at the double four-ring and unit cell level as well as its host–guest inclusion chemistry relating to advanced materials applications.

Acknowledgment. We (G.A.O., P.M.M., R.A.R.) are deeply indebted to the Natural Sciences and Engineering Research Council of Canada (NSERC) for generous financial support of this work. We are grateful to NSERC for graduate scholarships (C.L.B., S.J.K., A.M.M.) and acknowledge the Ontario Graduate Scholarship Programme for support of our research (M.R.S., T.J.). Technical assistance from and valuable discussions with Drs. Edith Flanigen, Steven Wilson, and Gregory Lewis, and Ms. Lisa King of UOP Tarrytown, NY are deeply appreciated.